Structures of Silicon-Doped Carbon Clusters

James L. Fye and Martin F. Jarrold*

Department of Chemistry, Northwestern University, 2145 Sheridan Road, Evanston, Illinois 60208

Received: September 9, 1996; In Final Form: December 10, 1996[⊗]

Gas phase ion mobility measurements have been used to examine the geometries of silicon-doped carbon cluster cations, C_nSi^+ ($n = 3-69$). The observed isomers resemble those found for pure carbon clusters: linear chains, monocyclic, bicyclic, and polycyclic rings, graphite sheets, and fullerenes. Generally, the silicon atom substitutes for a carbon atom and has only a minor effect on the structure. The linear chain and monocyclic ring isomers coexist for C_nSi^+ clusters over a wider range than for pure carbon cluster cations. The results provide the first conclusive experimental evidence that $C_{2n-1}Si^+$ fullerenes with an even number of atoms are closed-cage structures with the silicon atom networked into the cage. For $C_{2n}Si^+$ fullerenes with an odd number of atoms the silicon atom appears to be exohedral.

Introduction

When the now familiar icosohedral structure of buckminsterfullerene was proposed, it was recognized that the C_{60} cavity was capable of encapsulating an atom,[1] and a paper demonstrating lanthanum incorporation into fullerenes appeared only weeks later.[2] Early recognition that endohedral metallofullerenes provided a unique organometallic environment that may have interesting physical and chemical properties led to extensive theory[3] and gas phase characterization[4] of $M@C_{60}$ species. The implementation of the Krätschmer−Huffman method for production of bulk quantities of fullerenes[5] eventually led to an adaptation for the production of macroscopic amounts of endohedral fullerenes such as $La@C_{82}$.[6] In addition, the availability of bulk quantities of C_{60} allowed the preparation of exohedrally doped fullerenes in the gas phase[7] and solid phase.[8] The studies of endohedral and exohedral metallofullerene systems have been well documented elsewhere,[9] but a third doping possibility, heteroatom substitution into the cage structure, has received much less attention.

Replacing a fullerene carbon atom with a heteroatom results in a unique chemical site on the fullerene surface, which may be used as a reactive center or to modify the electronic properties. Transition metals and lanthanide metals have been shown to substitute into fullerene cages in the gas phase,[10] but more attention has been given to main group element substitution, with boron and nitrogen being of primary interest. Theoretical studies of $C_{59}B$ and $C_{59}N$ have predicted that they are stable, though with distorted fullerene cages.[11] Early gas phase experiments by Guo et al. demonstrated that boron could substitute into the fullerene cage to form $C_{60-x}B_x$ ($x \leq 6$).[12] Recently, Muhr et al. have reported the bulk production and extraction of $C_{59}B$ and $C_{69}B$ from boron-doped soot produced by the arc method.[13] The preparation of nitrogen-substituted fullerenes by conventional arc techniques has been more difficult,[14] but Hummelen et al. have been able to produce $C_{59}N$ synthetically, and they have isolated it as a $(C_{59}N)_2$ dimer.[15]

Silicon is another logical candidate for fullerene cage substitution. The isoelectronic substitution of silicon could potentially give a chemically distinct site in the cage, while minimizing the disturbance of the electronic properties. On the other hand, silicon substitution has potential complications resulting from the nature of silicon−carbon bonding interactions. Si−C bonds, which are typically 1.86 Å long for single bonds and 1.70 Å long for double bonds, will not easily fit into the C_{60} cage structure. In addition, silicon does not form the robust double bonds necessary for fullerene substitution, preferring instead to bond in an sp^3 tetrahedral configuration. Even with these disadvantages, the AM1 calculations of Bowser et al. predict that both single and double silicon substitution do not destabilize the C_{60} structure prohibitively.[16] But there has been no experimental confirmation of these predictions. Laser vaporization of silicon carbide (SiC) has been shown to produce C_{60} fullerene, and even in this greatly enriched silicon environment, no silicon-containing fullerenes were seen as products.[17] This implies that silicon-doped fullerenes may not form or at least will be difficult to isolate. Mass spectra of silicon-doped carbon clusters produced by laser vaporization of silicon and graphite composite targets has led to speculation about the existence of silicon-containing fullerenes, but direct information about the isomers present was not obtained in these studies.[18] Recently, Miller and West have produced bulk samples of $C_{58}Si_2$(oxides) and $C_{56}Si_4$(oxides) with yields of up to 1%, as determined by HPLC and mass spectrometry. The oxides presumably form at the reactive silicon site and are used here to trap the silicon-doped fullerene in a stable form.[19]

Although there is little information available on silicon-doped fullerenes, the study of small silicon/carbon clusters has been an active research area. The interest in these species is due to their probable role in the chemical vapor deposition of silicon carbide[20] and the identification of SiC_2[21] and SiC_4[22] in carbon stars. Detailed theoretical studies have predicted that SiC_2 is linear[23] and cyclic,[24] SiC_3 is cyclic,[25] and SiC_4 is linear.[26] Visible spectroscopy supports the cyclic geometry for SiC_2,[27] and linear SiC_4 has been identified by vibrational spectroscopy.[28] According to the calculations of Pascoli and Cameau, SiC_n^+ ($n = 1-5$) are linear.[29] This is in agreement with the conclusions of Parent[30] based on chemical reactivity studies but contradicts the conclusions of Negishi et al., who claim, also from chemical reactivity studies, that cyclic and linear structures coexist for $n = 2$ and 3, while $n = 4$ and 6 have linear structures and $n = 5$ is cyclic.[31] The coexistence of both linear and cyclic isomers has also been proposed to explain photoelectron spectroscopy results.[32]

In this paper we report studies of the geometries of silicon-doped carbon cluster cations using injected ion drift tube techniques. The results show that a variety of structural isomers are present for these clusters, including chains, rings, graphite

[⊗] Abstract published in *Advance ACS Abstracts,* February 15, 1997.

S1089-5639(96)02759-4 CCC: $14.00

sheets, and fullerenes. For the small clusters, linear chains and rings coexist. Clusters with an even number of atoms, $C_{2n-1}Si^+$, form fullerene structures with the silicon acting as a substitutional dopant for the missing carbon atom. For silicon-doped fullerenes with an odd number of atoms, $C_{2n}Si^+$, it appears that the silicon atom is exohedral.

Experimental Methods

Sample rods were prepared from mixtures of silicon powder (Aldrich, 99%) and graphite powder (Ultra Carbon, Ultra F) at 25:1 or 50:1 carbon to silicon atomic ratio. The mixture was dried at 450 K under vacuum, pressed into a pellet, and then transferred to the instrument. The experimental apparatus has been described in detail previously,[33] and only a brief overview will be given here. Clusters are generated by pulsed laser vaporization (308 nm) of the sample rod in a continuous flow of helium. Both pure carbon clusters, C_n^+, and silicon-containing carbon clusters, C_nSi^+, are produced. A high-energy electron beam is fired into the buffer gas approximately 1 cm from the exit aperture, to increase the number of ions leaving the source. After exiting the source, the cluster ions are focused into a quadrupole mass spectrometer. The mass-selected clusters are then focused into a low-energy ion beam and injected through a small aperture into the drift tube. The drift tube contains approximately 5 Torr of helium buffer gas, and ions travel across the drift tube under the influence of a weak electric field (13.2 V/cm). Isomers with compact geometries, and small orientationally averaged collision cross sections, experience fewer collisions with the helium buffer gas than more diffuse geometries with larger cross sections. Therefore, the compact isomers travel across the tube more rapidly, leading to a spatial and temporal separation of the geometric isomers.[34] The cluster ions that exit the drift tube through a small aperture are mass analyzed by a second quadrupole mass spectrometer and then detected by an off-axis collision dynode and dual microchannel plates.

Drift time distributions are recorded by injecting 50 μs pulses of cluster ions into the drift tube and recording the arrival time distribution at the detector with a multichannel scaler. The arrival time distribution is converted into a drift time distribution by correcting the time scale so that it only reflects the time spent traveling through the drift tube. Reduced mobilities were determined from the drift time distributions using[35]

$$K_0 = \frac{L}{t_d E}\frac{p}{760}\frac{273.15}{T} \quad (1)$$

where L is the length of the drift tube, t_d is the drift time, E is the electric field across the drift tube, p is the pressure in Torr, and T is the absolute temperature.

The isomer distribution can be annealed by increasing the injection energy of the cluster ions.[36] Collisions with the helium buffer gas initially heat and then quickly cool the clusters as they enter the drift tube. At high injection energies the clusters may become hot enough that they anneal or dissociate close to the entrance of the drift tube. Monitoring the drift time distribution and the mass spectrum of the ions exiting the drift tube as a function of injection energy provides information about the isomerization and fragmentation of the resolved isomers.

Results

Laser vaporization of the silicon−graphite target initially produces pure carbon clusters. After several hours, silicon-containing carbon clusters, C_nSi^+, grow to be 10−20% of the intensity of the pure carbon clusters. After prolonged laser vaporization, $C_nSi_2^+$ clusters also appear in the mass spectrum.

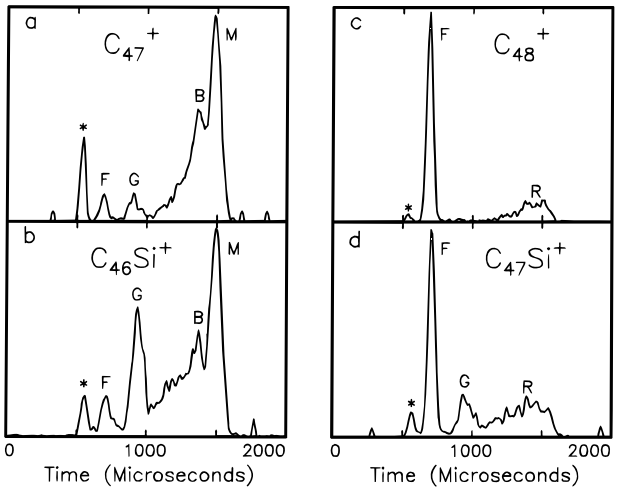

Figure 1. Drift time distributions for (a) C_{47}^+, (b) $C_{46}Si^+$, (c) C_{48}^+, and (d) $C_{47}Si^+$. The isomers are labeled F (fullerene), G (graphite sheet), B (bicyclic ring), M (monocyclic ring), R (unresolved rings), and * (doubly charged clusters).

Drift time distributions measured for C_{47}^+, C_{48}^+, $C_{46}Si^+$, and $C_{47}Si^+$ are shown in Figure 1. These drift time distributions were recorded with an injection energy of 150 eV. At this injection energy some annealing occurs so that the isomer distributions do not entirely reflect those generated by the source. The isomers observed for pure carbon clusters have previously been assigned by von Helden et al.[37] For C_{47}^+ the fullerene isomer (labeled F) appears at approximately 700 μs. The other features in this drift time distribution are assigned to graphite fragment (G), bicyclic ring (B), and monocyclic ring (M). The peak labeled with an asterisk at a shorter drift time than the fullerene peak is attributed to doubly charged C_{96}^{2+} fullerene. In the drift time distribution for C_{48}^+, the fullerene is more abundant, and the monocyclic and bicyclic rings (labeled R) are much less abundant. These results illustrate the strong odd−even alternation in the relative abundances of the isomers observed for the pure carbon clusters. The drift time distribution recorded for $C_{46}Si^+$ is very similar to that recorded for C_{47}^+, and the $C_{47}Si^+$ drift time distribution is very similar to that recorded for C_{48}^+. The close resemblance between drift time distributions recorded for C_{n+1}^+ clusters and C_nSi^+ clusters with the same total number of atoms is observed for all clusters studied, $n = 3-69$. The most significant difference is that the silicon-containing clusters display a slightly greater abundance of graphite fragment and polycyclic ring isomers.

The inverse reduced mobilities for the C_nSi^+ isomers resolved at low injection energies are plotted in Figure 2. The inverse mobilities are plotted here because they are directly proportional to the collision cross sections. Analogous results for the pure carbon clusters are shown in the figure by the line. The inverse mobilities for the silicon-doped carbon clusters, C_nSi^+, are slightly larger than those of the pure carbon clusters, C_{n+1}^+, with the same number of atoms, presumably because the silicon atom is larger than a carbon atom and because silicon−carbon bonds are longer than carbon−carbon bonds.

For pure carbon cluster cations, linear chains persist up to $n = 10$.[38] For C_nSi^+ clusters the linear chains persist to larger cluster sizes. However, it was difficult to determine how much larger. A substantial fraction of the linear C_nSi^+ clusters generated by the source contain hydrogen, despite considerable effort to remove this contaminant. Hydrogen stabilizes the linear chains. And because the mass resolution of our quadrupole mass spectrometers is 1 amu at best, it was difficult to determine when the pure C_nSi^+ chains disappeared. Linear chains were always observed up to $C_{12}Si^+$ and under some source conditions

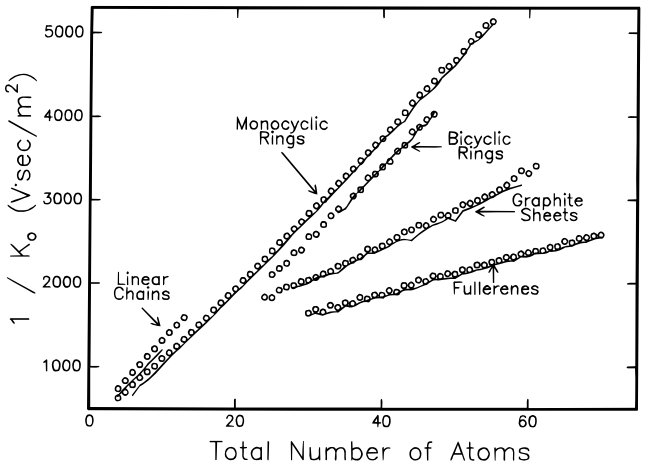

Figure 2. Inverse reduced mobilities for C_nSi^+ (○) and C_n^+ (—) isomers as a function of the total number of atoms in the cluster.

chains were present up to $C_{18}Si^+$. It is likely that the chains persist, with low abundances, to even larger sizes.

Monocyclic rings were resolved for C_nSi^+ clusters with $n = 3-55$. Larger monocyclic rings may exist, but they were not resolvable. Large monocyclic rings have also been observed for the pure carbon clusters. C_7^+ is the smallest carbon cluster cation to show a monocyclic ring, while the monocyclic ring persists for smaller C_nSi^+ clusters. Bicyclic rings, which are more difficult to resolve than most of the other isomers, begin to emerge as a shoulder on the monocyclic ring peak for C_n^+ and C_nSi^+ clusters with around 20 atoms. The bicyclic and polycyclic rings are generally more abundant for the silicon-containing clusters. Figure 2 shows only the bicyclic ring isomers that have been clearly resolved in these experiments. Clusters with more than 50 atoms have significant populations of bicyclic and polycyclic ring isomers that cannot be resolved. These large bi- and polycyclic rings are probably poorly resolved because there are many possible ring geometries with slightly different mobilities. The silicon-containing graphite sheet is more abundant than for the pure carbon clusters. Like the linear chain, the graphite sheet is also susceptible to hydrogen contamination, presumably because the addition of hydrogen atoms stabilizes this geometry.

Figure 3 shows a plot of the relative abundance of the fullerene isomers for C_n^+ and $C_{n-1}Si^+$ clusters, $n = 30-70$, as a function of the total number of atoms. There are strong odd−even alternations in the intensities. In both cases the fullerene isomer is more abundant for clusters where the total number of atoms is even. The lower relative abundances of the silicon-containing fullerenes relative to the pure carbon fullerenes reflect the significant graphite sheet population for the C_nSi^+ clusters.

Figure 4 shows a plot of the inverse reduced mobilities of the C_n^+ fullerenes and the C_nSi^+ fullerenes. The inverse mobilities for the pure carbon fullerenes increase approximately linearly with cluster size, with a slight pairing between the mobilities of the C_{2n}^+ and C_{2n-1}^+ fullerenes. The behavior of the silicon-containing fullerenes is similar, but the pairing is more pronounced. For the smaller silicon-containing fullerenes there are oscillations in the mobilities, and the inverse mobilities of the $C_{2n-1}Si^+$ fullerenes are larger than the inverse mobilities of the $C_{2n}Si^+$ fullerenes, even though the former has one fewer carbon atom. The inverse mobilities of the $C_{2n}Si^+$ fullerenes are significantly larger than for the pure carbon fullerenes with the same number of atoms.

Additional clues about the structure of the silicon-doped carbon clusters can be obtained from chemical reactivity experiments. A detailed examination of the chemical reactivity of these clusters was not performed. However, the silicon-doped

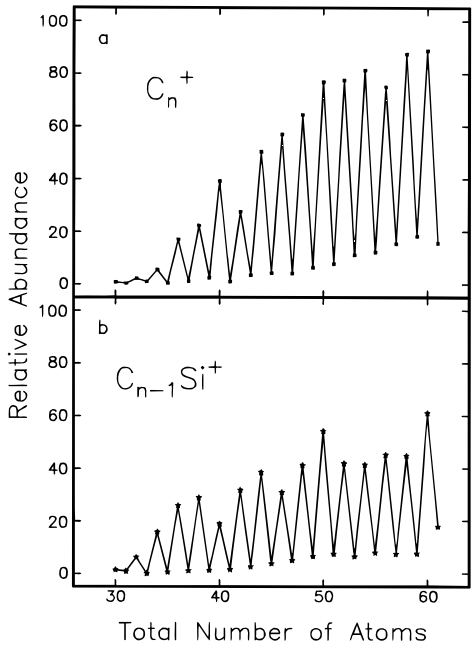

Figure 3. Relative abundance of the fullerene isomer for (a) C_n^+ and (b) $C_{n-1}Si^+$ as a function of the total number of atoms in the cluster. The line is added to clearly show the strong odd−even alternation in the fullerene population.

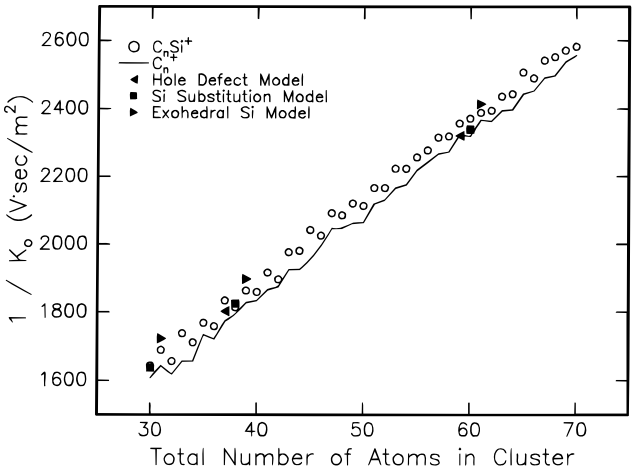

Figure 4. Inverse reduced mobilities of C_nSi^+ and C_n^+ fullerenes as a function of the total number of atoms in the cluster. Calculated mobilities of MNDO C_nSi model structures: hole defect ($n = 36$ and 58), silicon atom substitution ($n = 29$, 37, and 59), and exohedral silicon ($n = 30$, 38, and 60), are shown for comparison.

carbon clusters were observed to react readily with trace amounts of water in the drift tube to form adducts: $C_nSi^+\cdot(H_2O)_x$. Adducts with up to two water molecules form readily. Both the odd- and even-numbered clusters reacted at approximately the same rate to give analogous products. Drift time distributions were recorded for the monoadduct for some cluster sizes. They showed the same isomer population as the parent. Therefore, all the isomers appear to react at approximately the same rate.

Drift time distributions were recorded for C_nSi^+ with $n = 29$, 30, 39, 40, 49, 50, 59, and 60 as a function of injection energy to examine the annealing and dissociation of the silicon-doped carbon clusters. The observed behavior was very similar to that found for the pure carbon clusters. As the injection energy was raised, all the clusters examined showed an increase in the abundance of the monocyclic ring isomer and a corresponding decrease in the abundance of the polycyclic rings. For the larger clusters, the abundance of the ring isomers diminishes at higher injection energies, and the relative abundance of the

fullerene isomers increases. The relative abundance of the graphite fragment remains approximately unchanged. These results indicate that the ring isomers are isomerizing into fullerene isomers as the injection energy is increased. Similar behavior has been observed for the pure carbon clusters.[39]

As the injection energy is raised, some of the clusters fragment. The silicon atom is always included in the small neutral fragment that is produced. $C_{2n}Si^+$ clusters dissociate predominantly by loss of a $C_{2m}Si$ ($m = 0$, 1, and 2) neutral, while $C_{2n-1}Si^+$ clusters (except $C_{29}Si^+$) lose $C_{2m+1}Si$ ($m = 0$, 1, and 2). These dissociation pathways produce a carbon cluster cation with an even number of carbon atoms. The formation of a carbon cluster cations with an odd number of carbon atoms is generally a minor dissociation pathway. Odd-numbered product ions are more important in the fragmentation of $C_{2n-1}Si^+$ parent clusters. Unlike the pure carbon rings, dissociation by loss of C_{10}, C_{14}, and C_{18} products (which are believed to be aromatic rings) was not observed for the silicon-containing rings.

Discussion

There is a strong resemblance between drift time distribution measured for pure carbon clusters, C_n^+, and silicon-doped carbon clusters, $C_{n-1}Si^+$, with the same total number of atoms. This indicates that silicon effectively substitutes for a carbon atom, and silicon incorporation does not drastically affect the structural properties. The effect that this substitution has on the properties of the linear chain, monocyclic ring, and fullerene isomers will be discussed in more detail below with particular attention being paid to the silicon-containing fullerenes.

C_nSi^+ Chains and Rings. The linear chain persists to larger cluster sizes for C_nSi^+ clusters than for the pure carbon analogs. The existence of longer silicon-containing linear chains can be understood through simple bond energy and ring strain arguments. Calculations have shown that the lowes energy C_nSi linear chain has the silicon at the end of the chain.[26,29] In order for the linear chain to isomerize into a monocyclic ring, the energy gained by the formation of the new bond must overcome the strain energy generated by ring formation. Typical carbon−silicon single bonds are 0.2−1 eV weaker than carbon−carbon single bonds. Since the formation of a weaker carbon−silicon bond can compensate for less ring strain than a carbon−carbon bond, the linear C_nSi^+ isomer is expected to persist to larger cluster sizes. However, this is not the whole story because monocyclic ring isomer persists down to C_3Si^+, the smallest cluster studied, while for the pure carbon cluster cations the smallest ring observed was for C_7^+. Several theoretical studies have addressed the preferred geometry of small silicon-containing carbon clusters.[26,29] Though the details of the calculations vary, a consistent result is that the linear and cyclic isomers for small silicon-containing carbon clusters are close energetically. So the coexistence of these isomers over an extended size range is not surprising.

$C_{2n-1}Si^+$ Fullerenes with an Even Number of Atoms. The most likely candidate for structure of silicon-containing fullerenes where the total number of atoms is even, $C_{2n-1}Si^+$, is a closed-cage fullerene with the silicon atom substituting for a carbon atom in a C_{2n} cage. This geometry is supported by the strong odd−even alternations in fullerene abundance seen in Figure 3. Analogous odd−even alternations have previously been rationalized for the pure carbon clusters by proposing that the fullerenes with an even number of atoms can form closed-cage structures of five- and six-membered rings, while fullerenes with an odd number of atoms cannot. As a result, fullerenes with an odd number of atoms must contain a structural defect which makes it unstable toward reaction and/or dissociation.

The inverse mobilities for $C_{2n-1}Si^+$ fullerenes are slightly larger than their pure carbon analogs, presumably because of the longer Si−C bonds. Mobilities were calculated for silicon-substituted fullerenes, C_nSi^+ with $n = 29$, 37, and 59, to determine whether they were in agreement with the measured mobilities. The silicon-substituted fullerene geometries were obtained by replacing a carbon atom in an MNDO optimized fullerene. Clusters with $n < 40$ were then MNDO optimized, while for the larger cluster, a fragment was MNDO optimized and then the fullerene was reassembled. The bond lengths were then scaled by 0.988, a factor that brings the MNDO bond lengths of C_{60} into agreement with experiment. Mobilities were calculated using[35]

$$K_0 = \frac{(18\pi)^{1/2}}{16}\left[\frac{1}{m} + \frac{1}{m_b}\right]^{1/2} \frac{ze}{(k_B T)^{1/2}} \frac{1}{\Omega_{avg}^{(1,1)}} \frac{1}{N} \qquad (2)$$

where m and m_b are the masses of the ion and buffer gas, ze is the charge, N is the neutral number density at 760 Torr and 273.15 K, and $\Omega_{avg}^{(1,1)}$ is the orientationally averaged collision integral which was obtained from a rigorous hard-sphere scattering model[40] using hard-sphere contact distances of 2.81 Å for C−He collisions and 3.00 Å for Si−He collisions. The hard-sphere inverse mobilities calculated from the MNDO optimized structures are shown in Figure 4; they agree with the measured mobilities to within 1%. Thus, the measured mobilities are consistent with a silicon-substituted cage for $C_{2n-1}Si^+$ fullerenes with an even number of atoms.

$C_{2n}Si^+$ Fullerenes with an Odd Number of Total Atoms. There are three plausible structures for $C_{2n}Si^+$ fullerenes where the total number of atoms is odd: (1) C_{2n} fullerenes with a silicon attached to the outside of the cage—an exohedral silicon; (2) C_{2n} cages with a silicon inside the cage—an endohedral silicon; or (3) silicon-substituted fullerenes with a missing carbon atom—a hole defect. If the $C_{2n}Si^+$ fullerenes were C_{2n} cages with an endohedral silicon atom, the inverse mobilities of the $C_{2n}Si^+$ fullerenes and the C_{2n}^+ fullerenes should be very similar. Placing a silicon inside the cavity of a fullerene has little effect on the shape of the cluster and little effect on its orientationally averaged cross section. Thus, $Si@C_{2n}^+$ and C_{2n}^+ fullerenes would have essentially the same inverse mobilities. Examination of the data in Figure 4 clearly shows that $C_{2n}Si^+$ fullerenes have inverse mobilities that are 3−5% larger than the corresponding C_{2n}^+ fullerene. Furthermore, both $C_{2n}Si^+$ and $C_{2n+1}Si^+$ clusters react with trace amounts of water in the drift tube. An endohedral silicon would be protected from reaction by the closed carbon cage. Therefore, the presence of endohedral $Si@C_{2n}$ fullerenes is very unlikely.

For the hole-defect geometry, a pair of neighboring carbon atoms are removed from a C_{2n+2} fullerene, and the silicon atom resides in the hole, interacting with the dangling bonds of the four neighboring carbon atoms. An MNDO optimized structure for this geometry has four 1.9 Å Si−C bonds, which is consistent with a weak silicon−carbon single bond. This geometry has the advantage of avoiding an unfavorable Si═C double bond which is present in the silicon-substituted fullerene geometry for clusters where the total number of atoms is even. The hole-defect geometry could also be visualized as a $C_{2n+1}Si^+$ fullerene with a substituted silicon atom and one of the carbon atoms adjacent to the silicon removed. Thus, the collision cross section, and inverse mobility, for this geometry should be the same or possibly slightly smaller than those for the $C_{2n+1}Si^+$ silicon-substituted fullerenes. The data in Figure 4 show that for larger fullerenes, over 50 atoms, the qualitative expectations of this model are satisfied with the $C_{2n}Si^+$ inverse mobilities being generally slightly smaller than the inverse mobilities of the $C_{2n+1}Si^+$ fullerenes. But for small fullerenes, fewer than 50 atoms, the experimental results are inconsistent with the

predictions of the hole-defect structure. For the smaller fullerenes, between 30 and 40 atoms, the inverse mobilities for the $C_{2n+1}Si^+$ fullerenes are up to 2% smaller than the $C_{2n}Si^+$ fullerene even though they have one more atom. Therefore, the hole-defect model cannot explain all of the measured mobilities for the $C_{2n}Si^+$ fullerenes with an odd number of atoms, but it can explain those for the large clusters with 50 or more atoms.

An exohedral silicon atom is the only other plausible structure. Here we assume that a silicon atom bridges over a double bond on a closed C_{2n} carbon fullerene cage. Using a silicon bridged ethylene as a model system, MNDO optimization yielded 1.95 Å C−Si bonds, which are somewhat elongated from a typical 1.86 Å C−Si bond. The effect that an exohedral atom has on the mobility has been discussed in previous studies of metal-containing carbon clusters: It increases the collision cross section of the exohedral MC_{2n} by 6−8% over the C_{2n} fullerene.[10] As the cluster size increases, the increase in the inverse mobility, due to the exohedral atom, decreases. For an exohedral silicon atom, the inverse mobility is expected to increase by approximately 5% on going from a silicon-substituted $C_{29}Si^+$ fullerene to an exohedral $C_{30}Si^+$, and a 2% increase is expected on going from $C_{59}Si^+$ to $C_{60}Si^+$. This is in good agreement with the measured mobilities over the entire size range. Thus, the exohedral silicon model is the only model that can account for the inverse mobilities for the small C_nSi^+ fullerenes with an odd number of atoms. However, both the exohedral model and the hole-defect model can account for the mobilities of the larger, $n > 50$, fullerenes with an odd number of atoms. The main benefit of the hole-defect model is that insertion of the silicon atom into a two-carbon atom vacancy allows the cage to expand and reduce strain. The penalty is the breaking of the closed-cage bonding structure of the fullerene with the addition of only four weak C−Si bonds. The strain relief will be largest for the smaller fullerenes, which are clearly not hole defect structures but exohedral silicon structures. At larger sizes where the experimental data do not differentiate between the hole-defect and exohedral silicon structures, it seems unlikely that the silicon will insert to form the hole-defect structure since the main driving force, relief of strain, is greatly diminished.

Conclusions

We have used injected ion drift tube techniques to examine the structures of silicon-doped carbon clusters, C_nSi^+. The strong resemblance between pure carbon clusters and the silicon-doped carbon clusters indicates that the silicon acts as a substitutional dopant in the cluster, having only subtle effects on cluster's properties. The linear chain and monocyclic ring isomers coexist over a larger range of cluster sizes than for pure carbon clusters. The observation of rings as small as C_3Si^+ is consistent with theoretical predictions that the linear and cyclic structures are energetically competitive. The silicon atom also substitutes into fullerenes. $C_{2n-1}Si^+$ fullerenes with an even number of atoms appear to have the silicon atom substituting for a carbon atom in the cage, while fullerenes with an odd number of atoms appear to consist of a closed-cage carbon fullerene with an exohedral silicon atom.

Acknowledgment. We gratefully acknowledge the support of this work by the National Science Foundation (CHE-9306900) and the Petroleum Research Fund administered by the American Chemical Society.

References and Notes

(1) Kroto, H. W.; Heath, J. R.; O'Brien, S. C.; Curl, R. F.; Smalley, R. E. *Nature* **1985**, *318*, 162.

(2) Heath, J. R.; O'Brien, S. C.; Zhang, Q.; Liu, Y.; Curl, R. F.; Kroto, H. W.; Tittel, F. K.; Smalley, R. E. *J. Am. Chem. Soc.* **1985**, *107*, 7779.

(3) For example: Cioslowski, J.; Fleischmann, E. D. *J. Chem. Phys.* **1991**, *94*, 3730. Chang, A. H. H.; Ermler, W. C.; Pitzer, R. M. *J. Chem. Phys*. **1991**, *94*, 5004.

(4) For example: Cox, D. M.; Trevor, D. J.; Reichmann, K. C.; Kaldor, A. *J. Am. Chem. Soc*. **1986**, *108*, 2457.

(5) Krätschmer, W.; Lamb, L. D.; Fostiropoulos, K.; Huffman, D. R. *Nature* **1990**, *347*, 354.

(6) Chai, Y.; Guo, T.; Jin, C.; Haufler, R. E.; Chibante, L. P. F.; Fure, J.; Wang, L.; Alford, J. M.; Smalley, R. E. *J. Phys. Chem.* **1991**, *95*, 7564.

(7) For example: Weis, P.; Beck, R. D.; Bräuchle, G.; Kappes, M. M. *J. Chem. Phys.* **1994**, *100*, 5684.

(8) For example: Kortan, A. R.; Kopylov, N.; Ozdas, E.; Ramirez, A. P.; Fleming, R. M.; Haddon, R. C. *Chem. Phys. Lett.* **1994**, *223*, 501.

(9) Hirsch, A. *The Chemistry of the Fullerenes*; Thieme Verlag: Stuttgart, 1994.

(10) Clemmer, D. E.; Hunter, J. M.; Shelimov, K. B.; Jarrold, M. F. *Nature* **1994**, *372*, 248.

(11) Andreoni, W.; Gygi, F.; Parrinello, M. *Chem. Phys. Lett.* **1992**, *190*, 159. Chen, F.; Singh, D.; Jansen, A. *J. Phys. Chem.* **1993**, *97*, 10958. Wang, S.-H.; Chen, F.; Fann, Y.-C.; Kashani, M.; Malaty, M.; Jansen, A. *J. Phys. Chem.* **1995**, *99*, 6801.

(12) Guo, T.; Jin, C.; Smalley, R. E. *J. Phys. Chem.* **1991**, *95*, 4948.

(13) Muhr, H.-J.; Nesper, R.; Schnyder, B.; Kîtz, R. *Chem. Phys. Lett.* **1996**, *249*, 399.

(14) Pradeep, T.; Vijayakrishnan, V.; Santra, A. K.; Rao, C. N. R. *J. Phys. Chem.* **1991**, *95*, 10564. Yu, R.; Zhan, M.; Cheng, D.; Yang, S.; Liu, Z.; Zheng, L. *J. Phys. Chem.* **1995**, *99*, 1818.

(15) Hummelen, J. C.; Knight, B.; Pavlovich, J.; Gonzalez, R.; Wudl, F. *Science* **1995**, *269*, 1554.

(16) Bowser, J. R.; Jelski, D. A.; Xia, X.; Gao, J.; George, T. F. To be published.

(17) Koinuma, H.; Kim, M.-S.; Yoshimoto, M. *Jpn. J. Appl. Phys.* **1995**, *34*, 3720.

(18) Kimura, T.; Sugai, T.; Shinohara, H. *Chem. Phys. Lett.* **1996** *256*, 269.

(19) Miller, M.; West, R. Private communication.

(20) Borsella, E.; Aneve, L.; Fantoni, R.; Piccirillo, S.; Basili, N.; Enzo, S. *Appl. Surf. Sci.* **1989**, *36*, 213.

(21) Lucas, R.; GuÇlin, M.; Kahane, C.; Audinos, P.; Cernicharo, J. *Astrophys. Space Sci.* **1995**, *224*, 293.

(22) Ohishi, M.; Kaifu, N.; Kawaguchi, K.; Murakami, A.; Saito, S.; Yamamoto, S.; Ishikawa, S.-I.; Fujita, Y.; Shiratori, Y.; Irvine, W. M. *Astrophys. J.* **1989**, *345*, L83.

(23) Oddershede, J.; Sabin, J. R.; Diercksen, G. H. F.; Grüner, N. E. *J. Chem. Phys.* **1985**, *83*, 1702.

(24) Grev, R. S.; Schaefer, H. F., III *J. Chem. Phys.* **1984**, *80*, 3552.

(25) Alberts, I. L.; Grev, R. S.; Schaefer, H. F., III *J. Chem. Phys.* **1990**, *93*, 5046.

(26) Moazzen-Ahmadi, N.; Zerbetto, F. *Chem. Phys. Lett.* **1989**, *164*, 517.

(27) Michalopoulos, D. L.; Geusic, M. E.; Langridge-Smith, P. R. R.; Smalley, R. E. *J. Chem. Phys.* **1984**, *80*, 3556.

(28) Withey, P. A.; Graham, W. R. M. *J. Chem. Phys.* **1992**, *96*, 4068. Van Orden, A.; Provencal, R. A.; Giesen, T. F.; Saykally, R. J. *Chem. Phys. Lett.* **1995**, *237*, 77.

(29) Pascoli, G.; Cameau, M. *Astrophys. Space Sci*. **1995**, *226*, 149.

(30) Parent, D. C. *Int. J. Mass Spectrom. Ion Processes* **1992**, *116*, 257.

(31) Negishi, Y.; Kimura, A.; Kobayashi, N.; Shiromaru, H.; Achiba, Y.; Watanabe, N. *J. Chem. Phys.* **1995**, *103*, 9963.

(32) Nakajima, A.; Taguwa, T.; Nakao, K.; Gomei, M.; Kishi, R.; Iwata, S.; Kaya, K. *J. Chem. Phys.* **1995**, *103*, 2050.

(33) Jarrold, M. F.; Bower, J. E.; Creegan, K. J. *J. Chem. Phys.* **1989**, *90*, 3615.

(34) Hagen, D. F. *Anal. Chem.* **1979**, *51*, 870. St. Louis, R. H.; Hill, H. H. *Crit. Rev. Anal. Chem.* **1990**, *21*, 321. von Helden, G.; Hsu, M. T.; Kemper, P. R.; Bowers, M. T. *J. Chem. Phys.* **1991**, *95*, 3835.

(35) Mason, E. A.; McDaniel, E. W. *Transport Properties of Ions in Gases*; Wiley: New York, 1988.

(36) Jarrold, M. F.; Honea, E. C. *J. Am. Chem. Soc.* **1991**, *95*, 9181. Jarrold, M. F.; Constant, V. A. *Phys. Rev. Lett.* **1991**, *67*, 2994.

(37) von Helden, G.; Hsu, M.-T.; Gotts, N.; Bowers, M. T. *J. Phys. Chem.* **1993**, *97*, 8182

(38) von Helden, G.; Kemper, P. R.; Gotts, N. G.; Bowers, M. T. *Science* **1993**, *259*, 1300.

(39) Hunter, J. M.; Fye, J. L.; Jarrold, M. F. *Science* **1993**, *260*, 784. Hunter, J. M.; Fye, J. L.; Jarrold, M. F. *J. Phys. Chem.* **1993**, *97*, 3460. von Helden, G.; Gotts, N. G.; Bowers, M. T. *Nature* **1993**, *363*, 60. Hunter, J. M.; Fye, J. L.; Jarrold, M. F. *J. Chem. Phys.* **1993**, *99*, 1785.

(40) Shvartsburg, A.; Jarrold, M. F. *Chem. Phys. Lett.*, in press.